ICES Journal of Marine Science, 2022, **0**, 1–14
DOI: 10.1093/icesjms/fsac123
Original Article

Mapping habitat loss in the deep-sea using current and past presences of *Isidella elongata* (Cnidaria: Alcyonacea)

José Manuel González-Irusta [1,*], Joan E. Cartes [2], Antonio Punzón [1], David Díaz [3], Luis Gil de Sola [4] and Alberto Serrano [1]

[1]Instituto Español de Oceanografía, Centro Oceanográfico de Santander (COST-IEO), CSIC, Calle Severiano Ballesteros 16. 39004, Santander, Spain
[2]Institute of Marine Sciences (ICM-CSIC), Pg. Marítim de la Barceloneta 37–49, 08003 Barcelona, Spain
[3]Instituto Español de Oceanografía, Centro Oceanográfico de Baleares (COB-IEO), CSIC, Muelle de Poniente s/n, 07015 Palma de Mallorca, Spain
[4]Instituto Español de Oceanografía, Centro Oceanográfico de Malaga (COMA-IEO), CSIC, Puerto Pesquero, s/n Aptdo. 285 29640 Fuengirola, Spain

*Corresponding author: tel: +34 942291716; e-mail: jmanuel.gonzalez@ieo.csic.es

The bamboo coral *Isidella elongata* is an engineering species that forms a characteristic biogenic habitat in the bathyal mud of the Mediterranean Sea. This habitat has been severely reduced in recent decades due to trawling impacts, and there is a growing concern about its conservation status. In this work, the habitat loss of *I. elongata* was computed using a novel approach that combines the realized niche of the species with the estimation of its past distribution (before trawling) to delineate potential areas of habitat loss with different levels of uncertainty. The realized niche of the species was modelled using only live colonies and including trawling effort as explanatory variable whereas the past distribution was estimated also using the leftovers of dead colonies as presences. Trawling effort had a statistically significant negative effect on the extent of the realized niche of *I. elongata*, confirming previous results on the impact of this pressure on its distribution. The novel approach used in this work has allowed us to map for the first time several areas of potential habitat loss for *I. elongata* in the studied area, opening new opportunities to provide this essential information for future management and restoration actions of vulnerable marine ecosystems worldwide.

Keywords: coral gardens, habitat loss, Isidella elongata, potential niche, realized niche, trawling, VME.

Introduction

Habitat loss is considered a primary driver of natural ecosystems degradation and species extinction worldwide (Brooks *et al.*, 2002; Newbold *et al.*, 2015; Yeager *et al.*, 2020). In marine ecosystems, the direct impact of habitat loss is probably less extensive than that on land (although it is also less known) since its accessibility to human activities is lower. However, even in the most remote areas, such as the deep-sea, climate change, bottom trawling, oil and gas extraction, or deep-sea mining threatens natural biodiversity and habitat integrity (Morato *et al.*, 2006, 2020; Montagna *et al.*, 2013; Danovaro *et al.*, 2017; Dunn *et al.*, 2018; Boschen-Rose *et al.*, 2021). Of these activities, bottom trawling is the most widespread human activity affecting seabed habitats (Eigaard *et al.*, 2017; Hiddink *et al.*, 2017; Amoroso *et al.*, 2018). Trawling disturbance directly or indirectly affects benthic biodiversity, but its effects are especially severe for species with certain biological traits, such as sessile long-lived species (de Juan and Demestre, 2012; González-Irusta *et al.*, 2018; de Juan *et al.*, 2020; Dupaix *et al.*, 2021). Unfortunately, in the deep-sea, these are also traits of many habitat-former species (de la Torriente *et al.*, 2020), increasing the risk of habitat loss because of trawling disturbance (Reed *et al.*, 2007; Althaus *et al.*, 2009; Cartes *et al.*, 2013; Clark *et al.*, 2016), which has already been observed in previous reconstructions of past communities (Cartes *et al.*, 2017). In this context, a growing body of national and international legislation has been developed to protect deep-sea habitats and ecosystems. The United Nations General Assembly (UNGA) has adopted several Sustainable Fisheries Resolutions aiming to protect Vulnerable Marine Ecosystems (VMEs) in the high seas (Durán Muñoz *et al.*, 2012). At a European level, the EU has developed several directives, such as the Habitat Directive (HD, 92/43/EEC) or the Marine Strategy Framework Directive (MSFD, 2008/56/EC), aiming to protect marine benthic habitats as well as to limit habitat loss. More recently, the 2016/2336 regulation banned EU fleet bottom fishing at depths deeper than 800 m in the northeast Atlantic, limiting this activity in waters between 400 and 800 m in depth (van Denderen *et al.*, 2021), whereas in the Mediterranean Sea, trawling has been banned below 1000 m since 2006 (GFCM, 2006). Therefore, there is a growing interest in protecting and restoring (when needed) deep-sea benthic habitats, which to date has focused mainly on mapping and protecting (e.g. with Marine Protected Areas) their current distribution (e.g. Serrano *et al.*, 2017; Rodríguez-Basalo *et al.*, 2019; Torriente *et al.*, 2019), making efforts to map and quantify habitat loss much scarcer.

Isidella elongata (Esper, 1788) is a bamboo coral that forms a characteristic habitat on bathyal compact mud substrates with a depth distribution between 500 and 1200 m (Péres, 1967; Bellan-Santini, 1985), although our knowledge of its distribution and ecological requirements within this range is still scarce. This species is near endemic to the Mediterranean Sea, and its distribution area is limited to this en-

Received: March 4, 2022. **Revised:** June 2, 2022. **Accepted:** June 7, 2022

closed sea and the adjacent Atlantic Ocean in the Ibero-Moroccan Gulf (Grasshoff, 1988). However, bamboo corals (Fam. Isididae) are distributed worldwide in deep waters, often between depths of 200 and 1500 m, even reaching 2250 m and abyssal depths (Morris *et al.*, 2012). We can find >100 species of Isididae described, and most of them can probably be considered VME indicators, as described by Morato *et al.* (2018). Concerns on the conservation status of VME (Morato *et al.*, 2018) and specifically of *I. elongata* gardens have increased in this century, and in recent years, many studies have analysed different aspects of its ecology, including an analysis of its distribution and the effect of trawling disturbance on it (Maynou and Cartes, 2012; Cartes *et al.*, 2017; 2022; Lauria *et al.*, 2017; Mastrototaro *et al.*, 2017; Pierdomenico *et al.*, 2018; Carbonara *et al.*, 2020).

To turn these concerns into specific management actions, a better understanding of the current and past distribution of *I. elongata* is needed, including the delineation of areas where trawling disturbance has produced habitat loss. Future management efforts to enhance the natural recolonization of these areas (e.g. banning trawling) or even potential future efforts of ecological restoration (da Ros *et al.*, 2019) should consider the past natural distribution of such sessile fauna over the bottom. Therefore, it is crucial not only to analyse and quantify the effect of trawling disturbance on these habitats but also to reconstruct the past natural distribution of *I. elongata* on the seafloor. To better understand this, natural distribution would avoid local "introductions" of the species in places where it was never naturally found and/or probably would not develop well.

Unfortunately, directly determining reference conditions in heavily exploited ecosystems, such as the Mediterranean upper slopes (de Juan *et al.*, 2009; Eigaard *et al.*, 2017; Amoroso *et al.*, 2018), is not an easy task, and indirect estimation using distribution models (Elith and Leathwick, 2009; Reiss *et al.*, 2015) is often the only possibility. These models use statistical algorithms to correlate a set of explanatory variables, usually in a geographic information system (GIS) format, with a response variable, frequently the species distribution (Elith and Leathwick, 2009). Although these models normally use only environmental variables (e.g. depth, temperature, and slope) to explain marine benthos distribution, the recent growing availability of detailed fishing effort maps generated from GPS data (Eigaard *et al.*, 2017; Amoroso *et al.*, 2018) allows us to directly include trawling distribution in the models (González-Irusta *et al.*, 2018; Murillo *et al.*, 2020; Downie *et al.*, 2021b). The inclusion of fishing as another explanatory variable is not always possible because of data restrictions, but when available they allow to predict alternative scenarios with no fishing (González-Irusta *et al.*, 2018), which can be used to reconstruct baselines (Downie *et al.*, 2021b). Unfortunately, for species whose distribution is heavily affected by trawling, this approach could be biased by the range modification already generated by the pressure (Stirling *et al.*, 2016; Downie *et al.*, 2021a). In this work, we combined for the first time the use of distribution models with the use of past presences to delineate habitat loss for a biogenic habitat (the *I. elongata* coral gardens). The method present here has important management application globally and especially in Europe where the assessment of biogenic habitats under the MSFD include as criteria that the proportion of habitat loss does not exceed a specified percentage of its natural extent.

Material and methods

Study area

The study area extended from south of the Roses Gulf (Catalonia) to north of Nao Cape (Valencia), from ~41.25 to 38.25°N and 0 to 4°W (Fig. 1), in the Balearic Sub Basin (BSB). This area represents an old depression, the Valencia Trough, between the Valencia region and Catalan coasts in the Iberian Peninsula (mainland) and the Balearic Islands. The area is ~22700 km^2 with maximum depths at 2200–2300 m. The mainland has important tributary canyons and the Delta Ebro River plain, while the insular area presents narrow channels (across the islands) between the mainland and the southern open waters of the Algerian Basin. Both channels are the routes for the northward progression of surface warm fresh waters from the Alboran Sea–Algerian Basin and the southward progression of cold deep waters from the northern part of the BSB. In the studied areas, water masses are generally distributed at different depth belts, with a less saline and oxygen-rich surface water flowing southwards along the mainland shelf (Masó *et al.*, 1990) and two deeper main water layers in the domain of our target species: (i) the Levantine Intermediate Water (LIW) layer, distributed between 200 and 900 m, whose core is ~400 m, characterized to be more haline than surrounding waters; and (ii) the Western Mediterranean Deep Water (WMDW), below the LIW, filling all the Balearic Basin at depths >900 m (Pinot *et al.*, 2002). Another important feature in the area (northwestern Mediterranean) is the vertical flux of particles, arriving at deep waters (Miquel *et al.*, 2011), responsible for particulate organic matter (POM) arriving at the benthic boundary layer (BBL) and bottom sediments (Cartes and Figueroa, 2020).

Biological data

Biological samples were formed by a combination of different surveys performed since 1985 across the study area at depths ranging from 50 to 2300 m, with different sampling gear (mainly bottom otter trawls and less with beam trawls and sediment dredges; see Supplementary Table S1 for a summary). From the initial 1575 records, only 1127 were finally used after removing hauls with a geolocation error >6 km or located outside of the modelled area. Of these, 1065 were absences, whereas the other 62 had signs of the presence of *I. elongata*. The structure of this species is very fragile, and colonies are anchored by a wide white calcareous ramified base developed to support the structure of the colony. When the colony is affected by any fishing gear, it is usually broken by the first brown internodule, and the base with some internodule remains under the sediment in the surface layer. This species trait involves finding small internodules and spicules in the sediment after an impact and leaves a permanent sign of the presence in the sea bottom. This species trait can be used to record its presence years and even decades after it was removed from the sediment. From the 62 samples with signs of *I. elongata* presence, 36 were records of alive colonies, 24 had dead colonies and 2 were records of abundant sclerites found in muddy sediments.

Explanatory variables

An initial set of 12 potential explanatory variables available in a GIS format and considered relevant for driving the spatial distribution of *I. elongata* based on previous knowledge

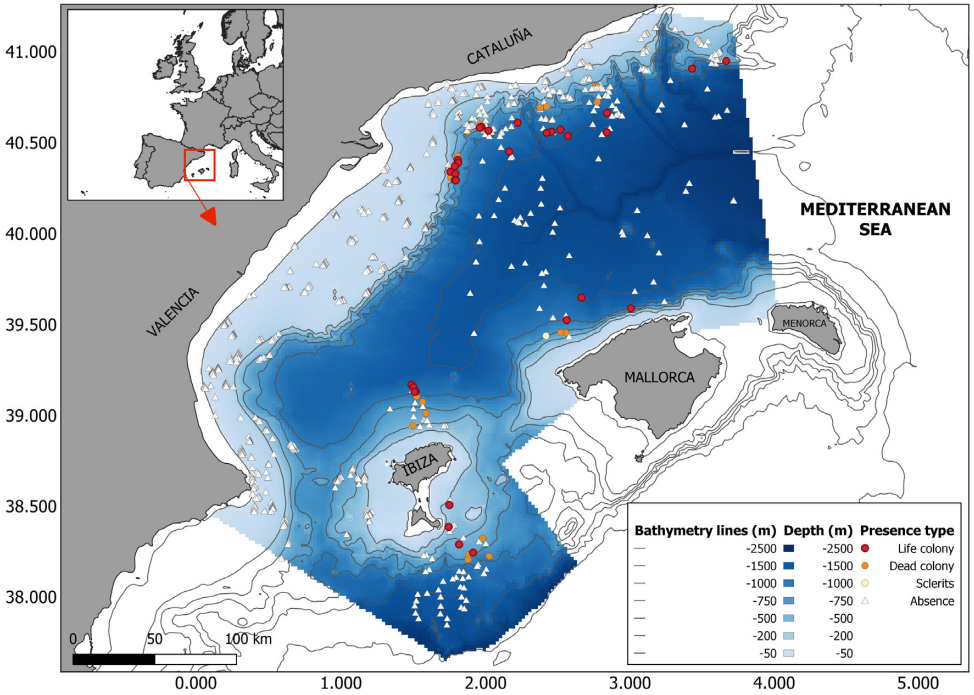

Figure 1. Sample distribution across the modelled area (in blue). The three types of presences are shown: live colonies (red circles), dead colonies (orange circles), and sclerites (yellow circles). Absences are represented as white triangles.

of the species (Cartes *et al.*, 2013; Lauria *et al.*, 2017; Pierdomenico *et al.*, 2018) were compiled and used as candidate predictors (Table 1). All variables were projected with the Lambert azimuthal equal-area projection and were rescaled using bilinear interpolation from their original resolution to a final resolution of 2 × 2 km (Supplementary Figure S1). Depth was computed after downloading the bathymetry data from EMODNET (http://www.emodnet-bathymetry.eu.) and rescaling it to the final projection and resolution using the function projectRaster (Hijmans, 2021) with bilinear interpolation. Terrain derivatives (slope, eastness, and northness) were computed from the rescaled depth using the terrain function (Hijmans, 2021). The Bathymetric Position Index (BPI) was computed using the rescale depth and the Benthic Terrain Model 3.0 tool in ArcGIS 10.1 (Walbridge *et al.*, 2018) with an inner radius of 3 and an outer radius of 25 grid cells. Terrain variables and BPI are probably some of the most common variables used in the field of distribution models for benthic species (e.g. Stirling *et al.*, 2016; Basalo *et al.*, 2019; de la Torriente *et al.*, 2018; Downie *et al.*, 2021b), including previous works on the distribution of *I. elongata* which also used terrain variables (Lauria *et al.*, 2017). The main reason for the recurrent use of these variables is that despite they are not directly linked to the biology of the species (as also occurs for depth) they are very good proxies (and quite often the only one available in a GIS format) to other relevant variables. Sediment type was extracted from the EMODNET portal (Vasquez *et al.*, 2021), whereas oceanographic variables (near-bottom temperature, near-bottom salinity, near-bottom currents and chlorophyll) were extracted from two oceanographic models publicly available on the Copernicus website (https://marine.copernicus.eu/). Salinity, temperature, and current velocities were computed as the mean value of monthly records for the period 2017–2020, extracted for each cell at the closest available depth (within the model) to the bottom. Both current velocities, *U* (from west to east) and *V* (from south to north), were extracted from the model "Mediterranean Sea analysis and forecast" (Clementi *et al.*, 2019), whereas the rest of the oceanographic variables (temperature, salinity, and chlorophyll) were extracted from the model "Mediterranean Sea Biogeochemical Analysis and Forecast" (Bolzon *et al.*, 2020). The original resolution for both models was 0.0417° (~4 km in the studied area). Both current velocities (*U* and *V*) were combined to compute the current intensity using the following formula:

$$Current\ intensity = \sqrt{(U\ velocity)^2 + (V\ velocity)^2}.$$

The surface chlorophyll values were computed as the mean value for each cell of the monthly records of the shallowest depth for the period 2017–2020 and were used as a proxy for the particulate organic carbon (POC) flux exported to the bottom. All computations were performed using different functions from the ncdf4 (Pierce, 2019) and raster (Hijmans, 2021) packages, including rescaling the layers from the model resolution to the final resolution. Finally, the maximum trawling effort for the period 2010–2020 was computed using the spatial distribution of the swept area obtained from the vessel monitoring system (VMS) and the logbook data. The VMS data (with the GPS location of the vessels recorded every 2 h) and the logbook data (with the technical characteristics of the boat, including the gear) were linked using the ship code and trip date fields. The VMS pings were cleaned using speed and other criteria to remove all pings not related to fishing, and then the swept area was computed annually for the studied period using cubic-hermite spline interpolation and adapting the width gear accordingly to each type of trawling present in the area (Hintzen *et al.*, 2010, González-Irusta *et al.*, 2018). According to Castro *et al.* (2007), we used a 20 m width gear for otter trawls (the information about gear type was also ob-

Table 1. Environmental data.

Variable	Source	Original resolution
Depth (m)	http://www.emodnet-bathymetry.eu.	≈115 × 115 m
Slope (degrees) and aspect (eastness and northness)	Obtained from depth after rescaling. Slope and aspect were obtained using the terrain function in the raster package (Hijmans, 2021). Eastness is the sin of aspect, whereas northness is the cos of aspect.	2 × 2 km
Bathymetric Position Index (BPI)	BPI was obtained using the Benthic Terrain Model 3.0 tool in ArcGIS 10.1 (ESRI, 2015) with an inner radius of 3 and an outer radius of 25 grid cells.	2 × 2 km
Salinity near bottom (‰)	Model: "*Mediterranean Sea Biogeochemical Analysis and Forecast*" (Bolzon *et al.*, 2020) downloaded from https://marine.copernicus.eu/.	0.0417° × 0.0417°
Temperature near bottom (°C)	Model: "*Mediterranean Sea Biogeochemical Analysis and Forecast*" (Bolzon *et al.*, 2020) downloaded from https://marine.copernicus.eu/.	0.0417° × 0.0417°
Chlorophyll (mg m^{-3})	Model: "*Mediterranean Sea Biogeochemical Analysis and Forecast*" (Bolzon *et al.*, 2020) downloaded from https://marine.copernicus.eu/.	0.0417° × 0.0417°
Current velocities: *U* and *V* vectors (m s^{-1})	Model: "*Mediterranean Sea analysis and forecast*" (Clementi *et al.*, 2019) downloaded from https://marine.copernicus.eu/.	0.0417° × 0.0417°
Trawling effort	Secretaría General de Pesca	0.05° × 0.05°

Summary of the explanatory variables included in the model.

tained from the logbooks). The final swept area was divided by the cell area to determine the number of times each area of the cell was totally trawled by year. The final raster included in the analysis was the maximum value in each pixel for the period 2010–2020 rescaled from the original resolution (0.05° × 0.05°) to the final resolution (2 × 2 km) using nearest neighbour interpolation. After compiling all the potential explanatory variables, the collinearity between them was evaluated using Pearson's coefficient of correlation and the variation inflation factors (VIFs, Zuur *et al.*, 2009). We retained a list of the most ecologically relevant variables with the Pearson coefficient of correlation <0.7 and with VIF values ≤3: depth, slope, northness, eastness, chlorophyll concentration, sediment type, trawling effort, and current intensity. In addition to these variables, we also included in the analysis the gear type with two levels: trawling gear (GOC73, OTSB-14, MTS-25) and dredge/sledge gear ("Box-corer", "Shipeck", "MacerGIROQ").

Data analysis

To compute habitat loss caused by bottom trawling, the suitable habitat of the species was modelled using two different approaches. (i) The first approach was focused on modelling the current distribution of *I. elongata* in the studied area, including the impact of bottom trawling on its current distribution (the "realized niche" approach). The current distribution of *I. elongata* was modelled using the locations of live colonies as presences and the rest of the sample points (including samples with dead colonies or sclerites) as absences. In this approach, trawling effort was included as an explanatory variable, and its impact on the suitable habitat of the species was quantified. (ii) The second approach was focused on modelling the potential historical distribution of *I. elongata* in the study area (the "fundamental niche" approach), using all records of *I. elongata*, including dead colonies and sclerite aggregations found in the sediment as presences and using pseudo-absences instead of real absences to avoid the impact of trawling on absence distribution. Pseudoabsence generation was performed by applying the same methodology described in Morato *et al.* (2020). In this second approach, gear type and trawling effort were not included as explanatory variables. In both approaches General Additive Models (GAMs) fitted with the mgcv package (Wood, 2011) were used. This technique is one of the most frequently used for model species distribution and can deal with both presence–absences and presence–pseudo-absences data (González-Irusta *et al.*, 2015; Morato *et al.*, 2020). In both cases, we used binomial GAMs, limiting the number of knots of the smoothing parameters to four to avoid overfitting. The full binomial model for the realized niche was

$$P_p = \beta_i + s\left(depth\right) + s\left(slope\right) + \left(trawling\ effort\right) + s\left(current\ velocity\right) + s\left(chorophyl\right) + s\left(northness\right) + s\left(eastness\right) + f\left(gear\right) + f\left(sediment\ type\right) + \varepsilon_i,$$

where P_p is the probability of finding live colonies of *I. elongata* using any of the sampled methods included in the analysis, β_i is the intercept, s is an isotropic smoothing function specific for each variable and model, f indicates variables included as factors, and ε_i is the residual error term. For the second option ("fundamental niche" approach), the full model was similar:

$$PSH = \beta_i + s\left(depth\right) + s\left(slope\right) + s\left(current\ velocity\right) + s\left(chorophyl\right) + s\left(northness\right) + s\left(eastness\right) + f\left(sediment\ type\right) + \varepsilon_i.$$

It is important to note that in this second approach, the dependent variable potential suitable habitat (*PSH*) was different from the dependent variable of the first approach (P_p). Whereas in the first approach, the variable modelled was the probability of finding live colonies of *I. elongata* (P_p, as a proxy for the realized niche), in the second approach, we used randomly generated pseudo-absences and all signs of *I. elongata* colonies (including dead colony remains and sclerites) as presences to model the *PSH* of *I. elongata* (as a proxy for its fundamental niche). Therefore, whereas in the first approach the dependant variable is the probability of finding *I. elongata* in a particular cell, in the second approach the dependant variable is the suitability index and not its probability since this depends on the prevalence, artificially modified in the second approach by the number of pseudo-absence generated (around 10000 in this work). In any case, both response variables were interpreted in this work as a proxy for suitable habitat to allow comparisons between them. In both approaches, we applied the same method to select the variables

ultimately included in the final models based on selecting the model (for each approach separately) with the lowest Akaike's information criteria (AIC) after building all possible models using the function dredge from the package MuMIn (Barton, 2020). The relative importance of each variable ultimately included in the models was tested by removing the targeted variable from the final model and computing the deviance variation.

Map generation

To map the *I. elongata* distribution and habitat loss produced by trawling impacts, the final GAMs (from both approaches) were applied to the GIS layers to generate two geographical predictions of the response variable of each model (P_p and *PSH*). A third prediction based on the first approach (predicting P_p values) but for an alternative "no-trawling" scenario was also computed by replacing trawling effort with zeros in the trawling effort layer (González-Irusta *et al.*, 2018; Downie *et al.*, 2021a). The standard error associated with each of these three predictions was also mapped, generating a final group of six maps, two predicting P_p values (with and without trawling effort), one predicting *PSH* values and another three with the standard error associated with these predictions. To obtain more comparable results between both approaches, the outputs of the second approach (the *PSH* prediction and its associated standard error) were multiplied by a correction factor obtained after dividing the prevalence of the data used in the first approach by the prevalence of the data used in the second approach, which was much lower because of the higher number of pseudo-absences. This correction did not modify the geographical distribution of the values but increased its range, made them more comparable between approaches and correcting the impact of the lower prevalence of the second approach because the generation of a great number of pseudo-absences (near 10.000).

The two predictions of P_p and the *PSH* prediction were then converted into binomial maps using a threshold. After checking several options, we used the value that maximizes kappa as a threshold because it offered the best balance between accuracy and overprediction. The threshold computation was made after correcting the values of the second approach, so the correction did not affect to extent of the binary maps. To limit the effect of threshold selection in the final outputs and to include prediction uncertainty in the map generation, a third value was added (uncertain prediction) to the binomial maps. Therefore, the final outputs showed three possible values: Suitable (the P_p or *PSH* is higher than the threshold even after removal its associated standard error from the prediction), uncertain (the P_p or *PSH* is higher or lower than the threshold depending on whether we add or extract the standard error), and unsuitable (the P_p or *PSH* is lower than the threshold even if we add the standard error to the prediction).

Based on these final outputs, two different approaches were applied to compute habitat loss. (i) **Habitat loss approach 1** was computed as the difference between both final P_p outputs ("real" and "no-trawling" scenarios) with three possible results: habitat loss low uncertainty (cells classified as suitable in the "no-trawling" scenario but classified as unsuitable in the "real" scenario), habitat loss high uncertainty (cells classified as suitable or uncertain in the "no-trawling" scenario but classified as uncertain or unsuitable, respectively, in the "real" scenario), and no habitat loss (all other possibilities). (ii) **Habitat loss approach 2** was computed as the difference between the P_p "real" scenario and the final output for *PSH*. The outputs of this map are the same as in the previous approach but replace the "no-trawling" scenario for the final output for potential distribution. All habitat loss computations were restricted to the trawling footprint. Finally, a final map of habitat loss was computed by merging both approaches.

Model evaluation

The models from both approaches were evaluated using a cross-validation method based on a random "block" selection of training and testing data (Guinotte and Davies, 2014; Morato *et al.*, 2020). First, we used the function spatialblock from the package blockCV (Valavi *et al.*, 2019) to generate two groups of spatially independent data using a checkboard strategy (see Valavi *et al.*, 2019 for more information on spatial block strategies). Then, each group was randomly assigned for training or testing purposes and subsampling (selecting 80% of the data of each group). This operation was repeated 10 times to compute five different statistical metrics: area under the curve (AUC) of the receiver operating characteristic, kappa statistic, specificity, sensitivity, and the true skill statistic (TSS). All the metrics that were threshold-dependent (all except AUC, see Fielding and Bell, 1997) were computed using the value that maximizes kappa as a threshold (the same metric used in the binomial map generation). Following Morato *et al.* (2020), we considered the overall accuracy of the model prediction good (AUC $>$ 0.8; TSS $>$ 0.6), moderate (0.7 $\leq$ AUC $\leq$ 0.8; 0.2 $\leq$ TSS $\leq$ 0.6), or poor (AUC $<$ 0.7; TSS $<$ 0.2) based on AUC and TSS. Furthermore, kappa outputs were interpreted following the scale of Landis and Koch (1977)) from fair ($>$0.2 & $\leq$0.4) to perfect ($>$0.8). Finally, the spatial autocorrelation in the residuals was analysed using variograms and the Moran test. No trends were observed in the variograms, and the *p*-values of the Moran test were $>$0.05 in all cases, so the spatial autocorrelation in the residuals was considered null.

Results

The realized and fundamental niches of *I. elongata* were modelled using GAMs, explaining 35.1 and 29.6% of the total deviance, respectively (Table 2). Of the five variables included in the first GAM (the proxy for the realized niche), four had significant effects on the probability of presence (P_p) of *I. elongata* (depth, slope, eastness, and trawling effort). Of these, eastness was the variable with the highest importance (higher delta deviance, Table 2), followed by depth, slope, and trawling effort. Slopes with orientations toward the west showed the lowest probability of the presence of *I. elongata* (Fig. 2). The effect of depth on P_p showed a maximum peak ~1100 m deep. Slope showed a positive linear effect on P_p, whereas trawling effort also showed a linear effect but with a negative slope (lower P_p for higher values of trawling effort). The final GAM for the second approach (proxy to the fundamental niche of *I. elongata*) included six variables (Table 2), all of which (except current intensity) had a statistically significant effect on the *PSH* of *I. elongata*. As was observed in the previous model, eastness was a very important variable together with chlorophyll concentration, slope and depth. The effect of

Table 2. GAM summary for both approaches (realized niche and potential niche), including explained deviance, final model formula, estimated degrees of freedom (edf), Chi-square, *p*-value, and delta deviance.

Variable	edf	Chi-square	*p*-value	Delta deviance
GAM for realized niche (35.1% deviance explained)				
$P_p = \beta_i + s(\text{depth}) + s(\text{eastness}) + s(\text{current intensity}) + s(\text{slope}) + s(\text{trawling effort}) + \varepsilon_i$				
Eastness	2.95	10.94	0.01	33.25
Depth	2.30	16.01	0.00	16.68
Slope	1.00	15.90	0.00	14.13
Trawling	1.00	6.84	0.01	10.27
Current intensity	1.75	1.91	0.43	3.55
GAM for potential niche (29.26% deviance explained)				
$PSH = \beta_i + s(\text{depth}) + s(\text{eastness}) + s(\text{northness}) + s(\text{slope}) + s(\text{current intensity}) + s(\text{chlorophyll}) + \varepsilon_i$				
Chlorophyll	2.94	37.53	0.00	59.26
Slope	2.94	22.89	0.00	44.98
Eastness	2.76	11.48	0.02	43.37
Depth	2.70	25.89	0.00	39.37
Northness	1.59	11.04	0.01	17.99
Current intensity	1.75	2.50	0.31	8.54

chlorophyll on the *PSH* showed a clear decrease after reaching values >0.15 mg m^{-3} in a similar way to the effect of eastness, which decreased gradually for values <0 (slopes orientated to the west). Furthermore, northness had a linear and positive effect on *PSH*, with the slopes facing north showing higher *PSH* values than the slopes facing south. The effects of slope on the response variable were different for the two models (i.e. the first and second approaches). For P_p, the effect was linear and positive, whereas for *PSH*, there was a peak at ~3.5°. These differences are shown in detail in Supplementary Figure S2 and were also observed for depth. Although depth showed a similar relationship with the response variable for both models, the depth peak at which the response variable was maximum differed between models, being shallower for the *PSH* (±850 m) than for the P_p (±1100 m).

The distributions of the P_p (for both the real and no-trawling scenarios) and the *PSH* of *I. elongata* across the study area are shown in Figure 3. All maps showed the highest values in the lower part of the slope between the bathymetry lines of 700 and 1000 m deep, although there were important geographical differences between them. Differences between maps of P_p for both scenarios (Figure 3a and b) are caused by trawling and therefore are limited only to areas affected by this pressure, mainly in the deeper part of the continental shelf and the upper part of the continental slope. These maps showed some of the highest values in the inner parts of the canyons of the Catalan coast (in slopes facing east), whereas the map for the *PSH* (Figure 3c) showed low values in these areas. Furthermore, whereas the maps for P_p showed high values for the lower part of the slope in the southwestern part of the study area, the map for the *PSH* showed low values. In general, the P_p maps are more optimistic than *PSH* map. Standard errors showed a positive correlation with the predictions and were generally higher in areas with higher predictions (Figure 3d–f). In maps showing P_p values, the standard error was high in the deeper parts of the prediction and in areas northeast of Mallorca as well as in the southeast of Ibiza, an area also highlighted as uncertain by the map of standard error for the *PSH* (3f). The predictions of suitable habitat in both approaches showed good (*PSH* outputs) or moderate (P_p outputs) performance for AUC and TSS according to the ranges previously described and moderate (*PSH* outputs) or fair (P_p outputs) according to the ranges for Kappa values (Table 3). The approach based on pseudo-absences showed significantly higher values in the *PSH* approach for all evaluated metrics except sensitivity (the capacity of the models to correctly predict presences), which was not significantly different.

Prediction and standard error maps from Figure 3 were combined to generate a map of the predicted suitable habitat of *I. elongata* as well as to compute areas of habitat loss using two different methods (Figure 4). Predictions of suitable areas in the realized niche approach for both real and no-trawling scenarios are shown in Figure 4a and b, respectively. Both maps show important differences within the trawling footprint, totally classified as unsuitable in the real scenario but with important suitable areas in the no-trawling scenario. Differences in suitable areas between the fundamental niche approach (Figure 4c) and the realized niche approach are more apparent, especially in the southwestern part of the study area.

Habitat loss because of trawling was computed using two different methods. In the first method (based exclusively on the fundamental niche approach), habitat loss was computed as the difference between the suitable habitat for the real scenario (Figure 4a) and the suitable habitat in the no-trawling scenario (Figure 4b). The areas of habitat loss were mainly concentrated in the deeper part of the trawling footprint, with the largest patch located in the southwestern part of the study area and along the Catalan coast, northwest of the Ebro delta. Some small areas were also located in the Balearic Islands slopes, eastern part of Ibiza Island (from north to south) and north of Mallorca. According to this method, 18.7% of the total suitable area of *I. elongata* in the studied area has been lost, although only 1.5% of this prediction was classified as of low uncertainty (Table 4). These values increased up to 42.4% of the suitable area when only depths shallower than 1000 m (maximum allowed depth for bottom trawling in the Mediterranean Sea) were included in the analysis. The second method to compute habitat loss was obtained as the difference between the suitable habitat for the fundamental niche approach (using the real scenario, Figure 4a) and the suitable habitat predicted using the potential niche approach (Figure 4c). In this second method, the habitat loss areas were much more concentrated along the Catalan coast, with smaller areas delineated in the southwestern part of the study area. As observed in the first method, there were also some areas of

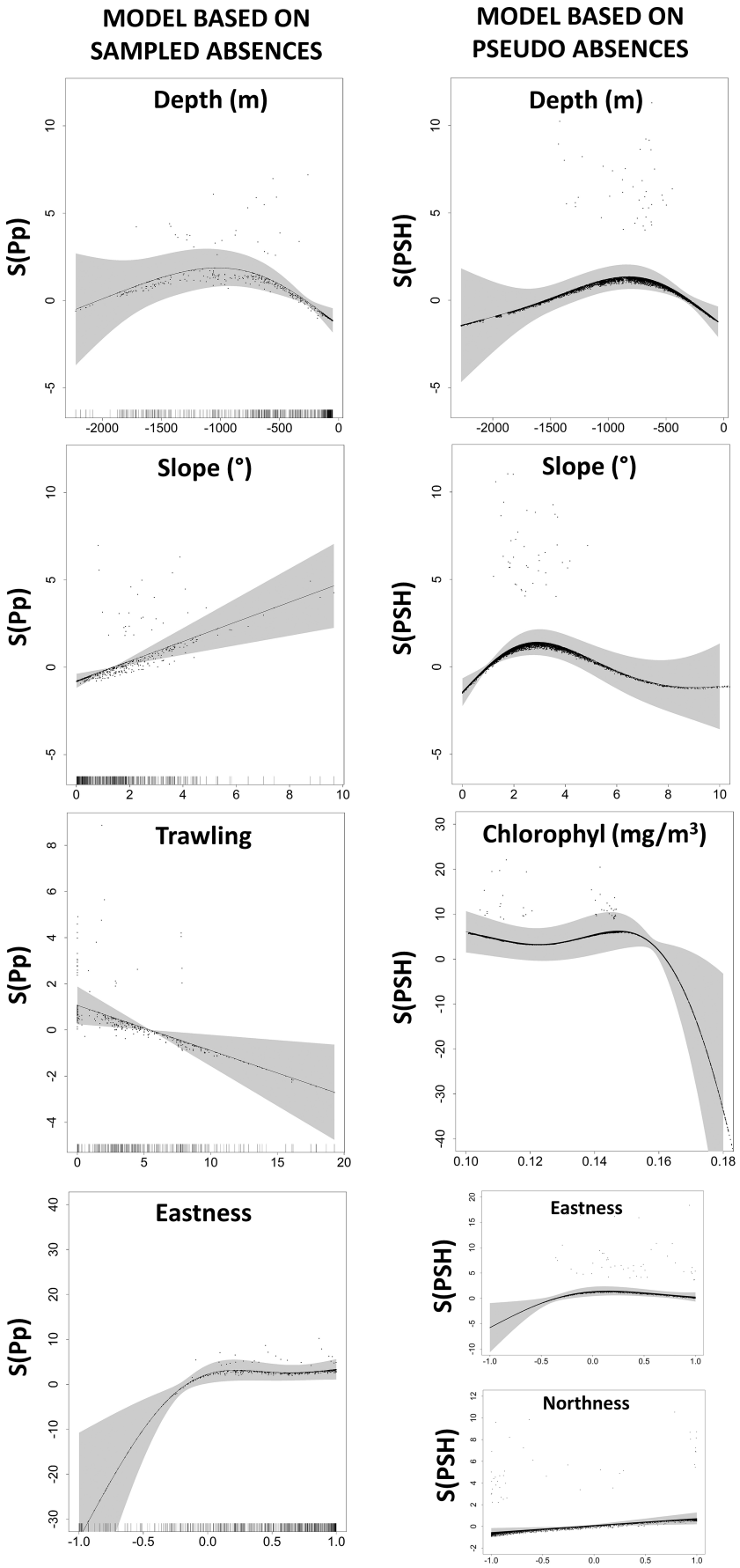

Figure 2. Response curves of the first approach (realized niche, left column) and the second approach (potential niche, right column). The shaded area represents the nominal confidence interval (95%) and the black dots are the residuals. Only variables with a significant effect are shown.

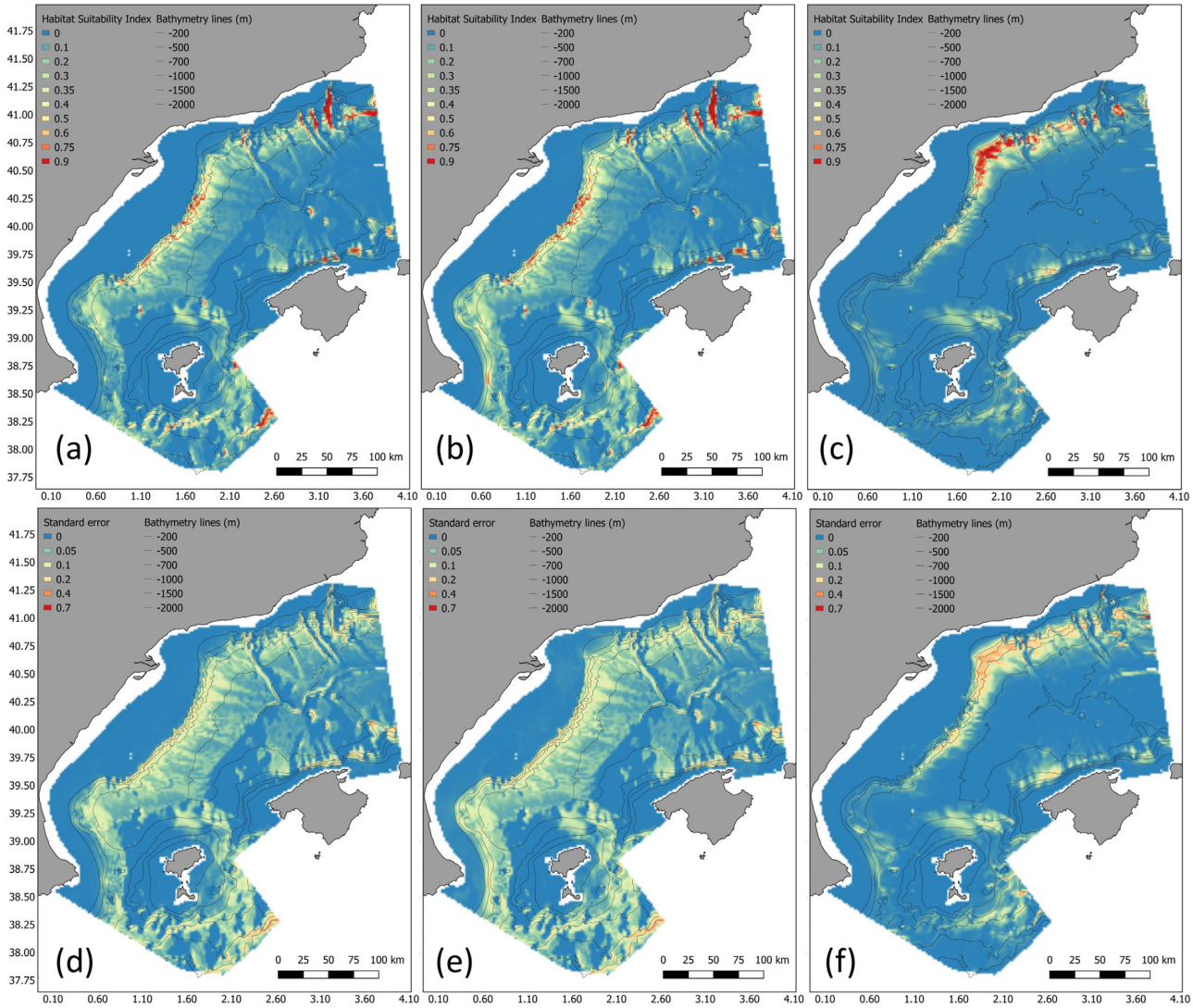

Figure 3. (a) Prediction of the Habitat Suitability Index (HSI) for the first approach (realized niche) using real trawling effort values. (b) Same as (a) after replacing the trawling effort values by zero. (c) Prediction of HSI for the second approach (potential niche). (d–f) Standard error associated with HSI predictions in (a), (b), and (c), respectively.

Table 3. Evaluation metrics for both approaches (realized and fundamental niche).

		AUC	Kappa	Sensitivity	Specificity	TSS
Realized niche		0.78 ± 0.06	0.16 ± 0.05	0.77 ± 0.17	0.73 ± 0.09	0.50 ± 0.10
Fundamental niche		0.88 ± 0.07	0.33 ± 0.21	0.73 ± 0.15	0.83 ± 0.13	0.57 ± 0.15
***t*-test**	***t***	−9.14	−3.19	−0.84	−3.64	−2.29
	df	16.88	10.2	17.8	16.55	16.28
	***p*-value**	<0.001	0.009	0.41	0.002	0.03

Area under the curve (AUC), True Skill Statistic (TSS). The values of both approaches (realized and fundamental niche) were compared using the Welch two samples *t*-test.

habitat loss around the Balearic Islands, although they were more abundant in this case. According to this second method, 24.4% of the total suitable area of *I. elongata* in the studied area has been lost, with 8.4% of this prediction classified as of low uncertainty (Table 4). As observed before, these values increased when only areas shallower than 1000 m are analysed, with values up to 59.4% of habitat loss for these areas. Finally, both methods to computed habitat loss were combined in a final map (Figure 5). This map showed three potential outputs of habitat loss. (i) Areas of habitat loss with low uncertainty (for cells classified as "habitat loss in both approaches and at least in one of them with low uncertainty) were located mainly west of the Ebro delta and across the Catalan coast, with some small patches in the southwest area and north of Mallorca. (ii) Areas of habitat loss with medium uncertainty (for cells classified as habitat loss in both approaches but with high uncertainty in both cases or only in one approach but with low uncertainty) were located around the cells of low uncertainty

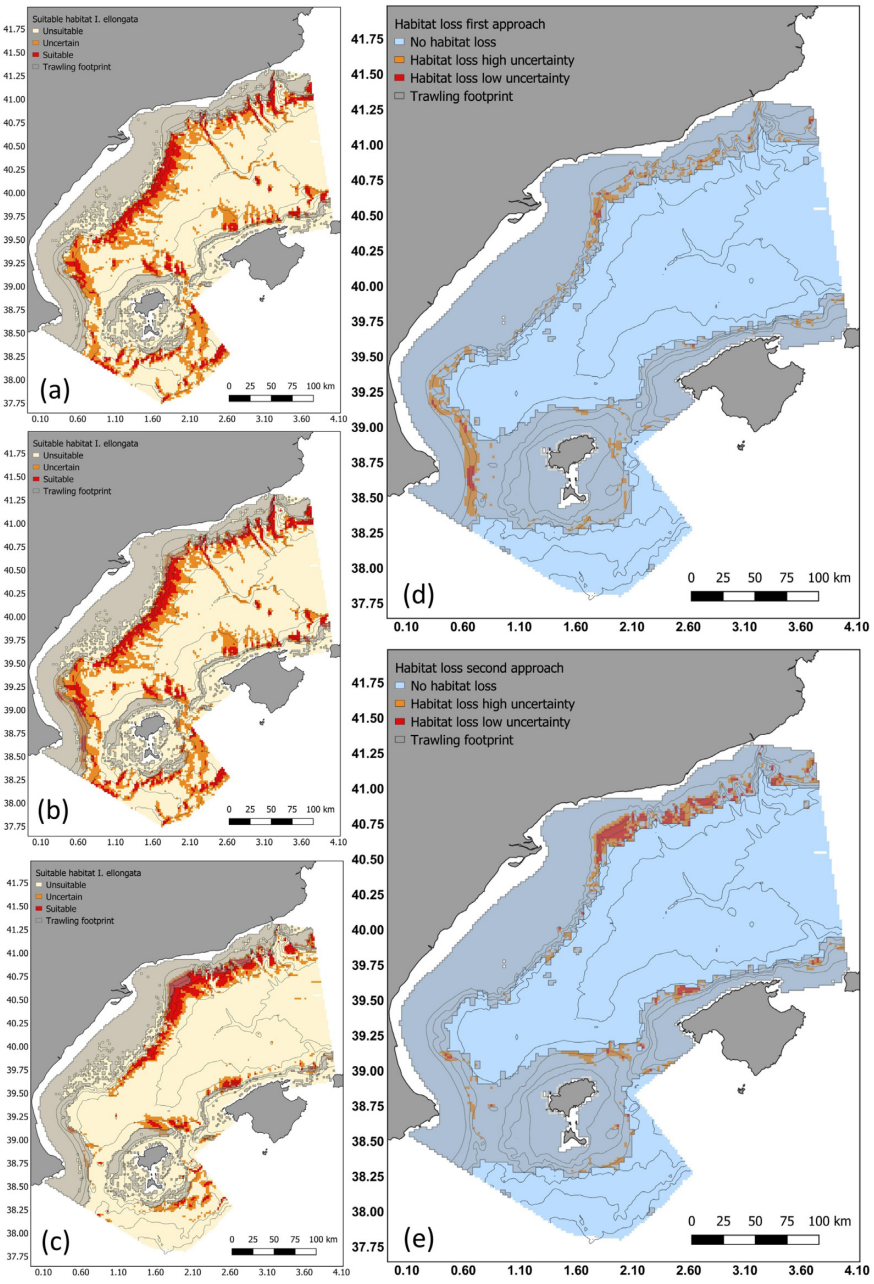

Figure 4. (a) Prediction of suitable habitat for the first approach (realized niche) using real trawling effort values. (b) Same as (a) after replacing the trawling effort values with zero. (c) Prediction of suitable habitat for the second approach (potential niche). (d) Habitat loss prediction computed as the difference between (a) and (b). (e) Habitat loss prediction computed as the difference between (a) and (c). Habitat loss was only computed inside the trawling footprint.

of the Catalan coast as well as in areas in the northern part of the Balearic Islands and south-west corner. (iii) Finally, areas of habitat loss with high uncertainty (for cells classified as "habitat loss with high uncertainty" in only one approach) were located mainly in the southwestern part of the study area with minor patches in the Catalan coast and the Balearic Islands. The predict values of habitat loss for both approaches combined was of 31.1% of the total suitable area, although 18.6% of this prediction was classified as of high uncertainty. These values increase up to 83.1% of habitat loss for the suitable areas located in the seabed shallower than 1000 m although again most of this prediction was considered highly uncertain (49.9%, Table 4).

Discussion

The current distribution of *I. elongata* in the Mediterranean Sea has been reduced by trawling disturbance (Maynou and Cartes, 2012; Cartes *et al.*, 2013; Lauria *et al.*, 2017; Pierdomenico *et al.*, 2018), and the study area is not an exception. Trawling effort had a negative and statically significant effect on the habitat suitability of this species, a result already described in Italian waters (Lauria *et al.*, 2017). Furthermore, the distribution of trawling impacts also seems to modify the observed relationship between the habitat suitability index and some environmental drivers, which showed different response curves between approaches. The depth niche of *I. elongata* was deeper in the realized niche (peaking at ~1000 m) than

Table 4. Area (km^2) and percentage (%) of habitat loss for each method.

		Area of habitat loss (km^2)	Habitat loss (%) for all suitable area	Habitat loss (%) for suitable area from 0 to 1 000 m
Habitat loss, first approach	High uncertainty	2 212	17,2	39,1
	Low uncertainty	188	1,5	3,3
	Total	2 400	18,7	42,4
Habitat loss, second approach	High uncertainty	2 200	16,0	38,9
	Low uncertainty	1 160	8,4	20,5
	Total	3 360	24,4	59,4
Both approaches combined	High uncertainty	2 820	18,6	49,9
	Medium uncertainty	1 396	9,2	24,7
	Low uncertainty	484	3,2	8,6
	Total	4 700	31,1	83,1

To compute the percentage, the area of habitat loss was divided by the sum of that area plus the suitable area predicted for current conditions (realized niche with real trawling effort).

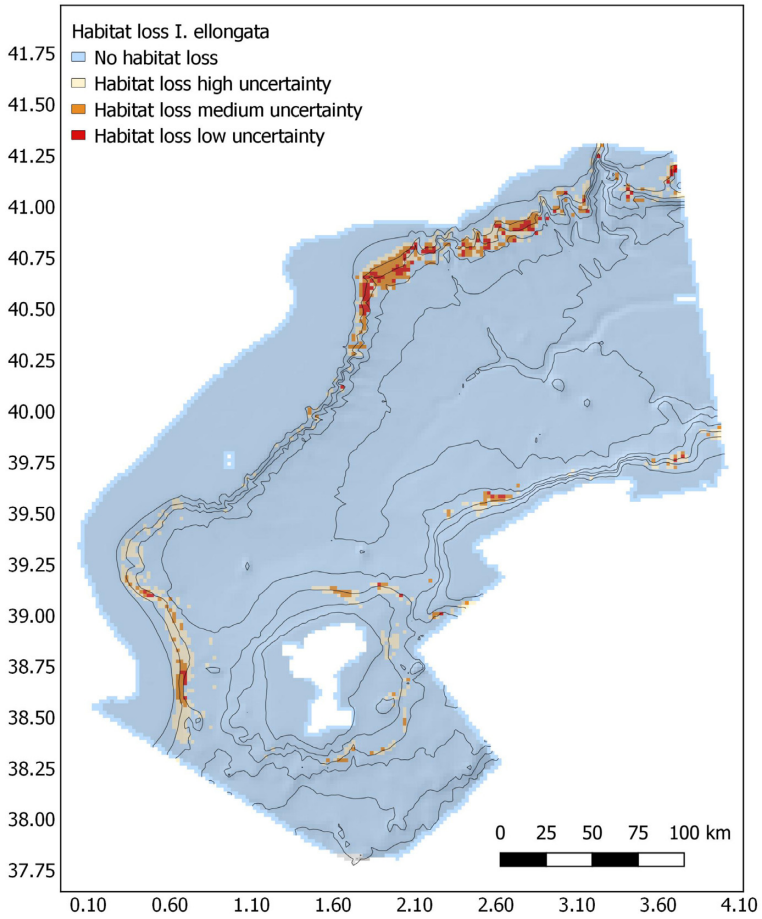

Figure 5. Final prediction of habitat loss in the studied area obtained by merging Figure 4d and e predictions, with four possible outputs: (i) no habitat loss (areas classified as no habitat loss in both figures); (ii) habitat loss with high uncertainty (for cells classified as "habitat loss with high uncertainty" in only one of the two figures); (iii) habitat loss with medium uncertainty (for cells classified as habitat loss with high uncertainty in both figures or for cells classified as habitat loss only in one figure but with low uncertainty); and (iii) habitat loss with low uncertainty (for cells classified as "habitat loss in both figures and at least in one of them with low uncertainty).

in the potential niche approach (peaking at ~800 m), and the slope preferences were also different between approaches. The preference for deeper and steeper slope seabed areas observed in the realized niche model may be a consequence of the removal of *I. elongata* from shallower, flat grounds, specifically targeted by trawlers in this area (Cartes *et al.*, 2013). A similar impact in the realized niche of other octocoral species as a consequence of trawling impacts has been recently described in the North Sea by Downie *et al.* (2021b). These authors analysed the realized niches of three species of sea pen in

the Greater North Sea and Celtic Seas, observing a low model transferability for *Funiculina quadrangularis* between the two areas because of differences in environmental preferences (especially in relation to muddy bottoms). The authors attributed these differences to the impact of trawling on the distribution of *F. quadrangularis* in the North Sea (and thus its effects on the relationship between the environmental drivers and the probability of presence). In a similar way, Stirling *et al.* (2016) found unexpected positive effect of ruggedness on the suitable habitat of the fan mussel, *Atrina fragilis* linking it with the negative impact of trawling on its distribution. To the best of our knowledge, until now, the impact of trawling on sensitive species using a distribution model has been assessed and mapped by replacing trawling effort with zero following the same method used in our first approach (González-Irusta *et al.*, 2018; Downie *et al.*, 2021a). Although this approach can offer very interesting and useful results in some cases, it can be biased when (as observed for *I. elongata*) the impact of trawling is so extreme that the whole distribution of the species (and not only its abundance) has been modified, restricting the species distribution to refuge areas with different environmental conditions. In these cases, the second approach used in this work can provide interesting and complementary results to the first approach by offering a proxy for the potential niche of the species (before the pressure) based on past presence records and pseudo-absence generation.

However, not all response curves show differences between approaches. Eastness showed a similar relationship with the response variable for all models, with a clear negative effect for values <0 (slopes with an orientation to the west). Along the tributary canyons occurring over the Catalan slope, we found the highest densities of *I. elongata* in flanks with northeast orientation, coinciding with the observed effects of both eastness and northness. Although these variables have not direct impact on species biology, they are recurrently used in distribution models of benthic species since they may act as good proxies to other relevant environmental variables such as current intensity or turbidity. In the Balearic Basin, intermediate and deep currents follow a general regime with a northeast to southwest direction (Pinot *et al.*, 2002; Millot, 2005). Since currents are not strong in the area (<0.3 m s^{-1}), direct exposure may be necessary to facilitate a minimum water flow through the polyps, which ensures sufficient food provision for *I. elongata*. Previous works have observed a positive effect of current on the probability of the presence of *I. elongata* (Lauria *et al.*, 2017). Furthermore, because of these general circulation patterns, canyons with a SW orientation may accumulate more sediment and turbidity than the NE flanks. This effect could help to explain the highest suitability of slopes with an eastern orientation. In fact, excess sedimentation may collapse polyp function (Erftemeijer *et al.*, 2012), as could occur after historical deforestation of the NW Iberian Peninsula with delta formations (Cartes *et al.*, 2013). However, it is important to highlight that the effects of eastness and northness on *I. elongata* distribution observed in this work are site dependent and not necessarily extrapolable outside our study area. Finally, the negative effect of sedimentation could also be linked to the negative effect of chlorophyll concentration observed in this work, since the negative impact is associated with values >0.15 mg m^{-3}. In the studied area, these values are only reached in coastal waters or far from the coast in areas associated with the Ebro River plume (see Supplementary Figure S1), rich in surface chlorophyll but also in sedimentation.

The predictive maps obtained using both approaches showed different outputs. The first approach (based on presence–absence) predicts a larger suitable extent for *I. elongata* than the second approach, contradicting the view that "only presence" models tend to overpredict in comparison with presence–absence models (Zaniewski *et al.*, 2002; González-Irusta *et al.*, 2015). Regardless of the accuracy of this assumption about "presence-only" models, it seems clear that in this work, the incomplete niche of *I. elongata* and the use of real absences from suitable areas affected by trawling is interfering in the discriminatory capacity of the first approach model, which provides more generous predictions of suitable habitat than the second approach, especially in the deepest areas and across the slope located in front of the Valencia coast. This was also observed in the evaluation metrics, which were significantly lower for all metrics except sensitivity (the capacity of the model to correctly predict presences), suggesting a poorer performance of this approach in terms of prediction accuracy.

These differences in the predictive outputs have an impact on the habitat loss computations and in the uncertainty of the combined approach, although interestingly, within the interest area (trawling footprint), the differences between both approaches are less apparent. In fact, similar patches across the studied area were mapped as areas of habitat loss in both approaches, including several patches across the Catalan slope, especially east of the Ebro delta, in a large area between Tarragona and Barcelona, several small patches located around Ibiza (especially in the eastern part of the island) and some small patches north of Mallorca. Both models predicted an important part of the suitable habitat of *I. elongata* in areas deeper than 1000 m and therefore outside the reach of bottom trawling, decreasing the proportion of total habitat loss to values lower than a third of the total area even when both approaches are combined. On the other hand, they both predicted important patches of habitat loss in the shallower part of the *I. elongata* niche at depths ranging from 500 to 1000 m, with some areas of high uncertainty located as shallow as 300 m. In these areas, the proportion of habitat loss increase to values >80% when both models are combined but caution is needed before use these values for quantitative exercises or to extract definitive conclusions about the total extent of habitat loss of *I. ellongata* in the area. It is important to highlight that this value will decrease to 33.3% of habitat loss if we remove areas predicted with high uncertainty (only classified as habitat loss in one of the methods). Further studies are needed to improve our understanding of the observed differences between approaches, helping to reduce uncertainty.

Biogenic habitats such as the *I. elongata* gardens are considered VMEs, making its protection a priority in the management of the deep-sea ecosystems. Despite this relevance, the efforts to assess its conservation status has been hindered globally by a lack of reference conditions that avoid assessing the extent of habitat loss suffered by these ecosystems. Because bottom trawling has been in place for decades, it is often very difficult to estimate the proportion of the biogenic habitat that has been lost, especially in the less well-known habitats from the deep-sea. This is not a minor problem since traditional risk assessment approaches based on the overlap of pressure layers with the distribution of the biogenic habitat or VME

indicator species will fail to find overlapping because of the habitat eradication from areas where the pressure occurs (de la Torriente *et al.*, 2022). Of course, only because the lack of overlapping cause by the impact of trawling in the distribution of sensitive species (Stirling *et al.*, 2016; González-Irusta *et al.*, 2018; Downie *et al.*, 2021a) is not possible to assume not impact. In fact, the lack of overlapping can be hiding a major impact, habitat loss (de la Torriente *et al.*, 2022), a fact that usually is ignored in management because the difficulty of reconstruct past distributions (Cartes *et al.*, 2017). In this work, we have mapped for the first time several areas of habitat loss of *I. elongata* in the eastern Spanish Mediterranean, a result of clear management relevance for the protection of this VME across the Mediterranean Sea. The results of this work allow to show the level of habitat loss suffered for this VME because of trawling in the studied area, providing different proportions of habitat loss with different levels of uncertainty. The map of habitat loss provided in this work identifies areas where management actions are required not only to protect current *I. elongata* patches but also to identify areas suitable for recovery and/or restoration, information especially relevant under the current context of reduction of trawling impacts on seabed habitats across Europe. Finally, it is important to highlight that the method applied in this work is potentially applicable in other areas (limited to the availability of the necessary information) to infer the past distribution of other VMEs, a necessary exercise to map habitat loss worldwide.

Supplementary Data

Supplementary material is available at the *ICESJMS* online version of the manuscript.

Author's contribution

JMGI, AS, and JC conceived the ideas; JMGI, AS, and JC designed methodology; JC, DD, AP, LGS, and JMGI collected and/or contributed pre-processed subsets of data; JMGI wrote code and analysed the data; and JMGI led the writing of the manuscript and all authors contributed critically to the drafts and gave final approval for publication.

Data availability statement

Data available on request.

Funding

The study was performed within and financed by the MICYT project RECOMARES (RTI2018-094066-B-I00) funded by Ministerio de Ciencia e Innovación, MICYIT.

Acknowledgments

Many colleagues participated in the cruise origins of the historic dataset used in this study. The authors want to thank all of them, including the crew members of all the vessels involved, mainly the crew of the R/V García del Cid.

References

Althaus, F., Williams, A., Schlacher, T. A., Kloser, R. J., Green, M. A., Barker, B. A., Bax, N. J. *et al.* 2009. Impacts of bottom trawling on deep-coral ecosystems of seamounts are long-lasting. Marine Ecology Progress Series, 397: 279–294.

Amoroso, R. O., Pitcher, C. R., Rijnsdorp, A. D., McConnaughey, R. A., Parma, A. M., Suuronen, P., Eigaard, O. R. *et al.* 2018. Bottom trawl fishing footprints on the world's continental shelves. Proceedings of the National Academy of Sciences, 115: 201802379.

Barton, K. 2020. MuMIn: Multi-Model Inference. R package version 1.43.17, https://CRAN.R-project.org/package=MuMIn.

Basalo, A., Delgado, F., Ortega, E., López, P., and Rodríguez, F. J. 2019. High resolution spatial distribution for the hexactinellid sponges *Asconema setubalense* and *Pheronema carpenteri* in the Central Cantabrian Sea. Frontiers in Marine Science, 8: 612761.

Bellan-Santini, D. 1985. The Mediterranean benthos: reflections and problems raised by a classification of the benthic assemblages. In Mediterranean Marine Ecosystems, pp. 19–48. Ed. by Moraitou-Apostolopoulou M.and and Kiortsis V.. Springer, Boston, MA.

Bolzon, G., Cossarini, G., Lazzari, P., Salon, S., Teruzzi, A., and Feudale, L. 2020. Mediterranean sea biogeochemical analysis and forecast (CMEMS MED-biogeochemistry 2018–2021). Copernicus Monitoring Environment Marine Service (CMEMS). Available at:https://marine.copernicus.eu/es, (last accessed date: 20 January 2022).

Boschen-Rose, R. E., Clark, M. R., Rowden, A. A., and Gardner, J. P. A. 2021. Assessing the ecological risk to deep-sea megafaunal assemblages from seafloor massive sulfide mining using a functional traits sensitivity approach. Ocean & Coastal Management, 210: 105656.

Brooks, T. M., Mittermeier, R. A., Mittermeier, C. G., da Fonseca, G. A. B., Rylands, A. B., Konstant, W. R., Flick, P. *et al.* 2002. Habitat loss and extinction in the hotspots of biodiversity. Conservation Biology, 16: 909–923.

Carbonara, P., Zupa, W., Follesa, M. C., Cau, A., Capezzuto, F., Chimienti, G., D´Onghia, G. *et al.* 2020. Exploring a deep-sea vulnerable marine ecosystem: *Isidella elongata* (Esper, 1788) species assemblages in the western and central Mediterranean. Deep Sea Research Part I: Oceanographic Research Papers, 166: 103406.

Cartes, J. E., Díaz-Viñolas, D., González-Irusta, J. M., Serrano, A., Mohamed, S., and Lombarte, A. 2022. The macrofauna associated to the bamboo coral *Isidella elongata*: to what extent the impact on Isideidae affects diversification of deep-sea fauna. Coral Reefs. Available at:https://link.springer.com/article/10.1007/s00338-022-02243-w.

Cartes, J. E., and Figueroa, D. F. 2020. Deep sea isopods from the western Mediterranean: distribution and habitat. Prog. Oceanogr, 188: 102415. https://doi.org/10.1016/j. pocean.2020.102415.

Cartes, J. E., Schirone, A., Barsanti, M., Delbono, I., Martínez-Aliaga, A., and Lombarte, A. 2017. Recent reconstruction of deep-water macrofaunal communities recorded in continental margin sediments in the balearic basin. Deep Sea Research Part I: Oceanographic Research Papers, 125: 52–64.

Cartes, J., LoIacono, C., Mamouridis, V., López-Pérez, C., and Rodríguez, P. 2013. Geomorphological, trophic and human influences on the bamboo coral *Isidella elongata* assemblages in the deep mediterranean: to what extent does Isidella form habitat for fish and invertebrates? Deep Sea Research Part I: Oceanographic Research Papers, 76: 52–65.

Castro, J., Abad, E., Artetxe, I., Cardador, F., Duarte, R., García, D., Hernández, C. *et al.* 2007. Identification and segmentation of mixed-species fisheries operating in the Atlantic Iberian Peninsula waters. Ibermix project. European commission. Directorate-General for Fisheries and maritime Affairs (Contract Ref.: FISH/2004/03-33).

Clark, M. R., Althaus, F., Schlacher, T. A., Williams, A., Bowden, D. A., and Rowden, A. A. 2016. The impacts of deep-sea fisheries on benthic communities: a review. ICES Journal of Marine Science, 73: i51–i69.

Clementi, E., Pistoia, J., Escudier, R., Delrosso, D., Drudi, M., Grandi, A., and Pinardi, N. 2019. Mediterranean sea analysis and forecast (CMEMS MED-Currents 2016–2019). Copernicus Monitoring Environment Marine Service (CMEMS). Available at:https://marine.copernicus.eu/es, (last accessed date 20 January 2022).

da Ros, Z., Dell'Anno, A., Morato, T., Sweetman, A. K., Carreiro-Silva, M., Smith, C. J., Papadopoulou, N. *et al.* 2019. The deep sea: the new frontier for ecological restoration.. Marine Policy, 108: 103642.

Danovaro, R., Corinaldesi, C., Dell'Anno, A., and Snelgrove, P. V. R. 2017. The deep-sea under global change. Current Biology, 27: R461–R465.

de Juan, S., and Demestre, M. 2012. A trawl disturbance indicator to quantify large scale fishing impact on benthic ecosystems. Ecological Indicators, 18: 183–190,

de Juan, S., Demestre, M., and Thrush, S. 2009. Defining ecological indicators of trawling disturbance when everywhere that can be fished is fished: a Mediterranean case study. Marine Policy, 33: 472–478.

de Juan, S., Hinz, H., Sartor, P., Vitale, S., Bentes, L., Bellido, J. M., Musumeci, C. *et al.* 2020. Vulnerability of demersal fish assemblages to trawling activities: a traits-based index. Frontiers in Marine Science, 7: 44.

de la Torriente, A., Aguilar, R., González-Irusta, J. M., Blanco, M., and Serrano, A. 2020. Habitat forming species explain taxonomic and functional diversities in a Mediterranean Seamount. Ecological Indicators, 118: 106747.

de la Torriente, A., Serrano, A., Fernández-Salas, L. M., García, M., and Aguilar, R. 2018. Identifying epibenthic habitats on the Seco de los Olivos Seamount: species assemblages and environmental characteristics. Deep Sea Research Part I: Oceanographic Research Papers, 135: 9–22.

de la Torriente Diez, A., González-Irusta, J. M., Serrano, A., Aguilar, R., Sánchez, F., Blanco, M., and Punzón, A. 2022. Spatial assessment of benthic habitats vulnerability to bottom fishing in a Mediterranean Seamount. Marine Policy, 135: 104850.

Downie, A-L., Piechaud, N., Howell, K., Barrio Froján, C., Sacau, M., and Kenny, A. 2021. Reconstructing baselines: use of habitat suitability modelling to predict pre-fishing condition of a vulnerable marine ecosystem. ICES Journal of Marine Science, 78: 2784–2796.

Downie, A., Noble-James, T., Chaverra, A., and Howell, K. 2021. Predicting sea pen (Pennatulacea) distribution on the UK continental shelf: evidence of range modification by benthic trawling. Marine Ecology Progress Series, 670: 75–91

Dunn, D. C., van Dover, C. L., Etter, R. J., Smith, C. R., Levin, L. A., Morato, T., Colaço, A. *et al.* 2018. A strategy for the conservation of biodiversity on mid-ocean ridges from deep-sea mining. Science Advances, 4: 1–16.

Dupaix, A., Mérillet, L., Kopp, D., Mouchet, M., and Robert, M. 2021. Using biological traits to get insights into the bentho-demersal community sensitivity to trawling in the Celtic Sea. ICES Journal of Marine Science, 78: 1063–1073.

Durán Muñoz, P., Sayago-Gil, M., Murillo, F. J., del Río, J. L., López-Abellán, L. J., Sacau, M., and Sarralde, R. 2012. Actions taken by fishing nations towards identification and protection of vulnerable marine ecosystems in the high seas: the Spanish case (Atlantic Ocean). Marine Policy, 36: 536–543.

Eigaard, O. R., Bastardie, F., Hintzen, N. T., Buhl-Mortensen, L., Buhl-Mortensen, P., Catarino, R., Dinesen, G. E. *et al.* 2017. The footprint of bottom trawling in european waters: distribution, intensity, and seabed integrity. ICES Journal of Marine Science, 74: 847–865.

Elith, J., and Leathwick, J. R. 2009. Species distribution models: ecological explanation and prediction across space and time. Annual Review of Ecology, Evolution, and Systematics, 40: 677–697.

Erftemeijer, P. L. A., Riegl, B., Hoeksema, B. W., and Todd, P. A. 2012. Environmental impacts of dredging and other sediment disturbances on corals: a review. Marine Pollution Bulletin, 64: 1737–1765.

Fielding, A. H., and Bell, J. F. 1997. A review of methods for the assessment of prediction errors in conservation presence/absence models. Environmental Conservation, 24: 38–49.

General Fisheries Commission for the Mediterranean. 2006. Report of the thirtieth session. Istanbul, Turkey, 24–27 January 2006. GFCM Report. No. 30. Rome,

González-Irusta, J. M., de la Torriente, A., Punzón, A., Blanco, M., and Serrano, A. 2018. Determining and mapping species sensitivity to trawling impacts: the BEnthos sensitivity index to trawling operations (BESITO). ICES Journal of Marine Science, 75: 1710–1721.

González-Irusta, J. M., González-Porto, M., Sarralde, R., Arrese, B., Almón, B., and Martín-Sosa, P. 2015. Comparing species distribution models: a case study of four deep sea urchin species. Hydrobiologia, 745: 43–57.

Grasshoff, M., 1988. Die Gorgonaria der expeditionen von Travailleur 1880–1882 und Talisman 1883 (Cnidaria, Anthozoa). Zoosystema 8: 9–38.

Guinotte, J. M., and Davies, A. J. 2014. Predicted deep-sea coral habitat suitability for the U.S. west coast. PLoS One, 9: e93918.

Hiddink, J. G., Jennings, S., Sciberras, M., Szostek, C. L., Hughes, K. M., Ellis, N., Rijnsdorp, A. D. *et al.* 2017. Global analysis of depletion and recovery of seabed biota after bottom trawling disturbance. Proceedings of the National Academy of Sciences, 114: 8301–8306.

Hijmans, R.J. 2021. Raster: geographic data analysis and modeling. R package version 3.5-2. https://CRAN.R-project.org/package=raster, (last accessed date: 20 January 2022).

Hintzen, N. T., Piet, G. J., and Brunel, T. 2010. Improved estimation of trawling tracks using cubic Hermite spline interpolation of position registration data. Fisheries Research. 101: 108–115.

Landis, J. R., and Koch, G. G., 1977, An application of hierarchical kappa-type statistics in the assessment of majority agreement among multiple observers. Biometrics, 33: 363–374.

Lauria, V., Garofalo, G., Fiorentino, F., Massi, D., Milisenda, G., Piraino, S., Russo, T. *et al.* 2017. Species distribution models of two critically endangered deep-sea octocorals reveal fishing impacts on vulnerable marine ecosystems in central Mediterranean Sea. Scientific Reports, 7: 1–14.

Masó, M., La Violette, P. E., and Tintore, J. 1990. Coastal flow modification by submarine canyons along the NE Spanish coast. Scientia Marina, 54: 343–348.

Mastrototaro, F., Chimienti, G., Acosta, J., Blanco, J., Garcia, S., Rivera, J., and Aguilar, R. 2017. *Isidella elongata* (Cnidaria: Alcyonacea) facies in the western Mediterranean Sea: visual surveys and descriptions of its ecological role. The European Zoological Journal, 84: 209–225.

Maynou, F., and Cartes, J. E. 2012. Effects of trawling on fish and invertebrates from deep-sea coral facies of *Isidella elongata* in the western Mediterranean. Journal of the Marine Biological Association of the United Kingdom, 92: 1501–1507.

Millot, C. 2005. Circulation in the Mediterranean Sea: evidences, debates and unanswered questions. Scientia Marina, 69: 5–21.

Miquel, J. C., Martín, J., Gasser, B., Rodriguez-y-Baena, A., Toubal, T., and Fowler, S. W. 2011. Dynamics of particle flux and carbon export in the northwestern Mediterranean Sea: A two decade time-series study at the DYFAMED site. Progress in oceanography, 91: 461–481.

Montagna, P. A., Baguley, J. G., Cooksey, C., Hartwell, I., Hyde, L. J., Hyland, J. L., Kalke, R. D. *et al.* 2013. Deep-sea benthic footprint of the deepwater horizon blowout. PLoS One,8: e70540.

Morato, T., González-Irusta, J., Dominguez-Carrió, C., Wei, C., Davies, A., Sweetman, A. K., Taranto, G. H. *et al.* 2020. Climate-induced changes in the suitable habitat of cold-water corals and commercially important deep-sea fishes in the North Atlantic. Global Change Biology, 26: 2181–2202.

Morato, T., Pham, C. K., Pinto, C., Golding, N., Ardron, J. A., Muñoz, P. D., and Neat, F. 2018. A multi criteria assessment method for identifying vulnerable marine ecosystems in the north–east Atlantic. Frontiers in Marine Science, 5: 1–13.

Morato, T., Watson, R., Pitcher, T. J., and Pauly, D. 2006. Fishing down the deep. Fish and Fisheries, 7: 24–34.

Morris, K.J., Herrera, S., Gubili, C., Tyler, P. A., , and Hauton, C. 2012, Comprehensive phylogenetic reconstruction of relationships in Octocorallia (Cnidaria: Anthozoa) from the Atlantic Ocean using mt-MutS and nad2 genes tree. Biogeosciences Discussions, 9: 16977–16998.

Murillo, F. J., Weigel, B., Bouchard Marmen, M., and Kenchington, E. 2020. Marine epibenthic functional diversity on flemish cap (north–

west Atlantic)—identifying trait responses to the environment and mapping ecosystem functions. Diversity and Distributions, 26: 460–478.

Newbold, T., Hudson, L. N., Hill, S. L. L., Contu, S., Lysenko, I., Senior, R. A., Börger, L. *et al.* 2015. Global effects of land use on local terrestrial biodiversity. Nature, 520: 45–50.

Péres, J. 1967. The Mediterranean benthos. In Oceanography and Marine Biology: An Annual Review. George Allen and Unwin, London .

Pierce, D. 2019. ncdf4: interface to unidata netCDF (Version 4 or earlier) format data files. R package version 1.17. https://CRAN.R-project.org/package=ncdf4, (last accessed date: 20 January 2022).

Pierdomenico, M., Russo, T., Ambroso, S., Gori, A., Martorelli, E., D'Andrea, L., Gili, J.-M. *et al.* 2018. Effects of trawling activity on the bamboo-coral *Isidella elongata* and the sea pen *Funiculina quadrangularis* along the Gioia Canyon (western Mediterranean, southern Tyrrhenian Sea). Progress in Oceanography, 169: 214–226.

Pinot, J-M., López-Jurado, J. L., and Riera, M. 2002. The CANALES experiment (1996–1998). Interannual, seasonal, and mesoscale variability of the circulation in the Balearic Channels. Progress in Oceanography, 55: 335–370.

Reed, J. K., Koenig, C. C., and Shepard, A. N. 2007. Impacts of bottom trawling on a deep-water oculina coral ecosystem off Florida. Bulletin of Marine Science, 81: 481–496.

Reiss, H., Birchenough, S., Borja, A., Buhl-Mortensen, L., Craeymeersch, J., Dannheim, J., Darr, A. *et al.* 2015. Benthos distribution modelling and its relevance for marine ecosystem management. ICES Journal of Marine Science, 72: 297–315.

Rodríguez-Basalo, A., Sánchez, F., Punzón, A., and Gómez-Ballesteros, M. 2019. Updating the master management plan for el cachucho MPA (Cantabrian Sea) using a spatial planning approach. Continental Shelf Research, 184: 54–65.

Serrano, A., González-Irusta, J. M., Punzón, A., García-Alegre, A., Lourido, A., Ríos, P., Blanco, M. *et al.* 2017. Deep-sea benthic habitats modeling and mapping in a NE Atlantic Seamount (Galicia bank). Deep Sea Research Part I: Oceanographic Research Papers, 126: 115–127.

Stirling, D. A., Boulcott, P., Scott, B. E., and Wright, P. J. 2016. Using verified species distribution models to inform the conservation of a rare marine species. Diversity and Distributions, 22: 808–822.

Torriente, A., González-Irusta, J. M., Aguilar, R., Fernández-Salas, L. M., Punzón, A., and Serrano, A. 2019. Benthic habitat modelling and mapping as a conservation tool for Marine Protected Areas: a seamount in the western Mediterranean. Aquatic Conservation: Marine and Freshwater Ecosystems, 29: 732–750,

Valavi, R., Elith, J., Lahoz-Monfort, J. J., and Guillera-Arroita, G. 2019. blockCV: an R package for generating spatially or environmentally separated folds for k-fold cross-validation of species distribution models. Methods in Ecology and Evolution, 10: 225–232.

van Denderen, P. D., Holah, H., Robson, L. M., Hiddink, J. G., Menot, L., Pedreschi, D., Kazanidis, G. *et al.* 2022. A policy-based framework for the determination of management options to protect vulnerable marine ecosystems under the EU deep-sea access regulations. ICES Journal of Marine Science, 79: 34–49.

Vasquez, M., Allen, H., Manca, E., Castle, L., and Lillis, H. 2021. EUSeaMap 2021. A European broad-scale seabed habitat map. https://archimer.ifremer.fr/doc/00723/83528/, (last accessed on 14 February 2022).

Walbridge, S., Slocum, N., Pobuda, M., and Wright, D. J. 2018. Benthic Terrain Modeler (BTM) 3.0, tools for understanding and classifying the benthic environment. [Sofware]. Esri, Redlands, CA.

Wood, S. N. 2011. Fast stable restricted maximum likelihood and marginal likelihood estimation of semiparametric generalized linear models. Journal of the Royal Statistical Society: Series B (Statistical Methodology), 73: 3–36.

Yeager, L. A., Estrada, J., Holt, K., Keyser, S. R., and Oke, T. A. 2020. Are habitat fragmentation effects stronger in marine systems? A review and meta-analysis. Current Landscape Ecology Reports, 5: 58–67.

Zaniewski, A. E., Lehmann, A., and Overton, J. M. C. 2002. Predicting species spatial distributions using presence-only data: a case study of native New Zealand ferns. Ecological Modelling, 157: 261–280.

Zuur, A. F., Ieno, E. N., Walker, N. , Saveliev, A. A., and Smith, G. M., Ebooks Corporation 2009. Mixed Effects Models and Extensions in Ecology with R. Springer, New York, NY. 574pp.

Handling Editor: Sasa Raicevich